

# Human MARCH1, 2, and 8 Block Ebola Virus Envelope Glycoprotein Cleavage via Targeting Furin P Domain

Chunfu Zheng<sup>1</sup>, Changqing Yu<sup>2</sup>, Wenbo Tan<sup>3</sup>, Yu Bai<sup>4</sup>, Yulong Zhou<sup>5</sup>, Jinbo Zhai<sup>6</sup>, Mengzhou Xue<sup>7</sup>, and Qiang Liu<sup>8</sup>

<sup>1</sup>Guangdong Academy of Agricultural Sciences

<sup>2</sup>Yibin Vocational and Technical College

<sup>3</sup>Heilongjiang University

<sup>4</sup>Wenzhou Vocational College of Science and Technology

<sup>5</sup>Heilongjiang Bayi Agricultural University

<sup>6</sup>Universities of Inner Mongolia Autonomous Region

<sup>7</sup>The Second Affiliated Hospital of Zhengzhou University

<sup>8</sup>Nanchong Vocational and Technical College

May 10, 2023

## Abstract

Membrane-Associated Ring-CH (MARCH) family proteins were recently reported to inhibit viral replication through multiple modes of action. Previous work proved that human MARCH8 blocked Ebola virus (EBOV) glycoprotein (GP) maturation. Our study here demonstrates that human MARCH1 and MARCH2 share a similar pattern to MARCH8 in restricting EBOV GP-mediated viral replication. Human MARCH1 and MARCH2 retain EBOV GP in the trans-Golgi network (TGN), reduce its surface display, and impair EBOV GP-pseudotyped virions infectivity. Furthermore, we uncover that the host proprotein convertase (PC) furin could interact with human MARCH1/2 and EBOV GP intracellularly. Importantly, the furin P domain is confirmed to be recognized by MARCH1/2/8, which is critical for their blocking activities. Besides, bovine MARCH2 and murine MARCH1 also impair EBOV GP proteolytic processing. Altogether, our findings confirm that MARCH1/2 proteins of different species showed a relatively conserved feature in blocking EBOV GP proteolytic processing, which could provide a reference for subsequent antiviral studies and may facilitate the development of novel strategies to antagonize enveloped virus infection.

## Human MARCH1, 2, and 8 Block Ebola Virus Envelope Glycoprotein Cleavage via Targeting Furin P Domain

Changqing Yu <sup>1</sup> #, Wenbo Tan <sup>4</sup> #, Yu Bai <sup>5</sup> #, Yulong Zhou <sup>8</sup>, Jingbo Zhai <sup>6</sup>, Mengzhou Xue <sup>7</sup>, Chunfu Zheng <sup>2,9</sup>\*, Qiang Liu <sup>3</sup>\*

<sup>1</sup> Engineering Center of Agricultural Biosafety Assessment and Biotechnology, School of Advanced Agricultural Sciences, Yibin Vocational and Technical College, Yibin, People's Republic of China;

<sup>2</sup> Institute of Animal Health, Guangdong Academy of Agricultural Sciences, Key Laboratory of Livestock Disease Prevention of Guangdong Province, Scientific Observation and Experiment Station of Veterinary Drugs and Diagnostic Techniques of Guangdong Province, Ministry of Agriculture and Rural Affairs, Guangzhou, People's Republic of China;

<sup>3</sup> Nanchong Key Laboratory of Disease Prevention, Control and Detection in Livestock and Poultry, Nanchong Vocational and Technical College, Nanchong, People's Republic of China;

<sup>4</sup> College of Advanced Agriculture and Ecological Environment, Heilongjiang University, Harbin, People's Republic of China;

<sup>5</sup> College of Animal Science, Wenzhou Vocational College of Science and Technology, Wenzhou, People's Republic of China;

<sup>6</sup> Key Laboratory of Zoonose Prevention and Control at Universities of Inner Mongolia Autonomous Region, Medical College, Inner Mongolia Minzu University, Tongliao, People's Republic of China;

<sup>7</sup> Department of Cerebrovascular Diseases, The Second Affiliated Hospital of Zhengzhou University, 2 Jingba Road, Zhengzhou, Henan, People's Republic of China;

<sup>8</sup> College of Animal Science and Technology, Heilongjiang Bayi Agricultural University, Daqing, People's Republic of China;

<sup>9</sup> Department of Microbiology, Immunology & Infection Diseases, University of Calgary, Calgary, Alberta, Canada.

# These authors contributed equally to this work.

\* Correspondence

Chunfu Zheng, zheng.alan@hotmail.com

Qiang Liu, liuqiang\_yyy@163.com

**Abstract:** Membrane-Associated Ring-CH (MARCH) family proteins were recently reported to inhibit viral replication through multiple modes of action. Previous work proved that human MARCH8 blocked Ebola virus (EBOV) glycoprotein (GP) maturation. Our study here demonstrates that human MARCH1 and MARCH2 share a similar pattern to MARCH8 in restricting EBOV GP-mediated viral replication. Human MARCH1 and MARCH2 retain EBOV GP in the trans-Golgi network (TGN), reduce its surface display, and impair EBOV GP-pseudotyped virions infectivity. Furthermore, we uncover that the host proprotein convertase (PC) furin could interact with human MARCH1/2 and EBOV GP intracellularly. Importantly, the furin P domain is confirmed to be recognized by MARCH1/2/8, which is critical for their blocking activities. Besides, bovine MARCH2 and murine MARCH1 also impair EBOV GP proteolytic processing. Altogether, our findings confirm that MARCH1/2 proteins of different species showed a relatively conserved feature in blocking EBOV GP proteolytic processing, which could provide a reference for subsequent antiviral studies and may facilitate the development of novel strategies to antagonize enveloped virus infection.

## KEYWORDS

MARCH proteins, Ebola virus, furin, envelope glycoprotein, cleavage

## 1 INTRODUCTION

Currently, a group of host cell membrane-associated proteins has been discovered to target viral envelope glycoproteins, including IFN-induced transmembrane (IFITM) proteins, serine incorporator (SERINC) and MARCH proteins (1). These cellular innate immunity factors could exert their antiviral activities at multiple stages of viral replication.

Originally, MARCH proteins were identified to show homology with the E3 ubiquitin ligase of K3 and K5 of the Kaposi's sarcoma-associated herpesvirus (KSHV) (2, 3). The MARCH family proteins now have been extended to comprise at least 11 members, most of which share a similar molecular structure, including a cytoplasmic N-terminal C4HC3 RING-finger (RING-CH finger) domain and two or more transmembrane domains, except for MARCH7 and MARCH10, which contain no predicted transmembrane domains. MARCH family proteins are widely involved in cell surface protein regulation (3-9), innate immunity signal transduction (10-12) and autophagy pathways regulation (13-15). MARCH1 and MARCH2 were originally found to downregulate the transferrin receptor (TfR) and CD86 (B7-2) (3). MARCH1 was able to mediate MHC II ubiquitination and thus promote dendritic cell selection of natural T regulatory cells (16). In addition,

MARCH1 could inhibit type I IFN signaling pathways (17). MARCH2 recognized syntaxin-6 (18), regulated secretory proteins trafficking (19), and negatively regulated cell autophagy (20) and NF- $\kappa$ B essential modulator (NEMO) signaling (21).

Recently, MARCH proteins were found to show antiviral activities (22, 23). Tada et al. first reported that MARCH8 could inhibit HIV-1 and VSV-G pseudotyped virus infection by targeting their envelope glycoproteins (24). Subsequently, MARCH1 and MARCH2 were also found to inhibit viral replication potentially (25-28). The viral proteins targeted by MARCH proteins now are extended to envelope glycoproteins of EBOV (27, 29, 30), severe acute respiratory syndrome coronavirus 2 (SARS-CoV-2) (27, 28, 30), murine leukemia virus (MLV) (24, 27), influenza virus (IAV) (27, 29, 31), Nipah virus (NiV) (27), spring viremia of carp virus (SVCV) (32) and rabies virus (RABV) (28), M2 protein of IAV (33), and N protein of porcine epidemic diarrhea virus (PEDV) (15). Interestingly, in contrast to the negative role on viral replication, MARCH8 was also critically supportive of hepatitis C virus (HCV) replication (34).

Generally, two antiviral modes are employed by MARCH proteins to restrict viral replication. On one side, MARCH proteins downregulated viral envelope glycoproteins expression and induced their intracellular degradation, which was the viral protein *c* ytoplasmic *t* ail*d* ependence (CTD), including envelope glycoproteins of VSV and RABV, and M2 protein of IAV (24, 28, 33). On the other side, MARCH proteins retained viral envelope glycoproteins at intracellular compartments without degradation, which relied on their E3 ubiquitin ligase activities but was the viral protein *c* ytoplasmic *t* ail *i* ndependence (CTI), including envelope glycoproteins of HIV-1, EBOV, and SARS-CoV-2 (24, 29, 30, 35).

EBOV GP is critical for its target cell infection. EBOV GP<sub>0</sub> precursor experiences initial N-glycosylation modification in the endoplasmic reticulum (ER) and is then transported to the trans-Golgi network (TGN), where it finishes its mature N- and O-glycosylation (36). The mature N, O-glycosylated GP<sub>0</sub> is cleaved into two subunits (GP<sub>1</sub> and GP<sub>2</sub>) by furin protease at the highly conserved polybasic sites (R-X-A/R-R) (36). The GP<sub>1</sub> and GP<sub>2</sub> subunits are re-linked via disulfide bonds and form GP<sub>1,2</sub> (37), assembled into self-trimers, and transported to the cell membrane. GP<sub>1</sub> contains a mucin-like domain (MLD), which is both N-glycosylated and highly O-glycosylated and thus dramatically increases its molecular weight. Therefore, the molecular weight of the mature glycosylated GP<sub>1</sub> is usually a little larger than the full-length immature glycosylation form GP<sub>0</sub>.

It was previously reported that human MARCH8 retained EBOV GP at TGN and blocked its proteolytic cleavage via targeting furin under the CTI antiviral pattern (29). Here, we extend to investigate the anti-EBOV GP activities of human MARCH1/2, bovine MARCH1/2, and murine MARCH1/2. Our results show that human MARCH1 and MARCH2, bovine MARCH2, and murine MARCH1 could inhibit EBOV GP intracellular cleavage. Critically, human MARCH1 and MARCH2 are also found to hijack furin, as MARCH8 did, to block EBOV GP activities, demonstrating a conserved CTI antiviral mode among MARCH molecules and thus shedding light on subsequent antiviral studies.

## 2 METHODOLOGY

### 2.1 Cell lines

Human embryonic kidney 293T cells, cervical cancer HeLa cells, human liver Huh-7 cells, and African green monkey kidney Vero cells were cultured at 37°C, and 5% CO<sub>2</sub> in DMEM (Gibco) supplemented with 8% fetal bovine serum (FBS) (Gibco), streptomycin, and penicillin (100  $\mu$ g/ml). All cell lines were obtained from the American Type Culture Collection (ATCC).

### 2.2 DNA constructs

The bovine MARCH1/2 and murine MARCH1/2 genes were obtained from bovine/murine peripheral blood mononuclear cells (PBMC) through RT-PCR amplification and cloned into the pCAGGS vector with the C-terminal HA tag by EcoRI/XhoI restriction sites. The human MARCH8 was provided by professor Kenzo Tokunaga (pCAGGS-3 $\times$ HA-MARCH8) or cloned into the pCAGGS vector with a C-terminus HA tag (pCAGGS-MARCH8-HA). The human MARCH1 and MARCH2 were synthesized and cloned into the

pCAGGS vector (pCAGGS-MARCH1/2-HA) according to the GenBank deposited sequences (GenBank accession #NM\_001166373 and #NM\_016496). Human/bovine/murine MARCH1-GFP and MARCH2-GFP expression vectors were constructed by inserting MARCH1 or MARCH2 into the pEGFP-N1 vector (GenBank accession #U55762) via EcoRI/AgeI restriction sites. Human MARCH1/MARCH2 was cloned into the pcDNA3.1-VN vector by EcoRI/AgeI restriction sites, generating the pcDNA3.1-MARCH1/MARCH2-VN. The N-terminal HA-tagged EBOV GP $\Delta$ MLD expression vector was produced via site-directed mutagenesis using FLAG-tagged EBOV GP $\Delta$ MLD as the backbone (29). The N-terminal FLAG-tagged EBOV GP $\Delta$ MLD and full-length EBOV GP were cloned into pcDNA3.1(+) expression vector based on their parental vectors (29). The VSV-G expression vector, Furin/Furin- $\Delta$ CD (furin CD deletion)/Furin- $\Delta$ P (furin P deletion) expression vectors, MARCH8-GFP/EBOV GP- $\Delta$ MLD-GFP expression vectors, Furin-VC/MARCH8-VN/GP- $\Delta$ MLD-VC expression vectors, calnexin-mCherry /TGN46-mCherry expression vectors, and pNL-Luc- $\Delta$ Env proviral reporter vector were used as previously described (29).

### 2.3 Confocal microscopy assay

HeLa cells ( $2 \times 10^5$ ) were seeded on glass slides 10 h before transfection. The HeLa cells were transfected with Lipofectamine 3000 reagent (Thermo Fisher). Twenty-four hours later, the cells were washed, fixed with 4% paraformaldehyde, and permeabilized with 0.1% Triton X-100. After washing, the cells were blocked with 5% bovine serum albumin (BSA). Cells were incubated with an anti-HA primary antibody for 1 h at RT for the immunofluorescence assay. After 3 washes, cells were stained with an Alexa Fluor 647-conjugated secondary antibody for 1 h at RT. Following 3 washes with PBS, cells were stained with DAPI for 30 min, washed for 1 h at RT, and used for confocal microscopy assay (ZEISS LSM700). At least 100 random cells per slide were analyzed, and the most representative images from each slide were selected for presentation.

### 2.4 Flow cytometry assay

To detect BiFC, the pcDNA3.1-MARCH1-VN/MARCH2-VN/MARCH8-VN, and Furin-VC expression vectors were co-transfected into 293T cells. After 36 h, the 293T cells were collected and used for flow cytometry analysis.

### 2.5 Western blot (WB) assay

293T cells ( $5 \times 10^5$  or  $2 \times 10^6$ ) were seeded in 6-well plates or 10 cm dishes 12 h before transfection. Thirty-six hours post-transfection, the cells were lysed with radioimmunoprecipitation assay (RIPA) buffer (Sigma) and cleared by centrifugation. Then, the supernatants were collected, mixed gently with loading dye, and boiled in a water bath for 5 min. Subsequently, the samples were subjected to sodium dodecyl sulfate-polyacrylamide gel electrophoresis (SDS-PAGE) and transferred to a polyvinylidene difluoride (PVDF) membrane, which was blocked with 4% nonfat milk for 1 h at RT. After washing, the membrane was incubated with the primary antibody and horseradish peroxidase (HRP)-conjugated secondary antibody. Alternatively, the membrane was directly incubated with an HRP-conjugated primary antibody. Finally, the PVDF membrane was exposed to enhanced chemiluminescence (ECL).

### 2.6 Antibodies

Mouse anti-actin, mouse anti-HA, and mouse anti-FLAG monoclonal antibodies were purchased from Sigma. HRP-conjugated anti-mouse immunoglobulin G secondary antibodies were purchased from Pierce. Alexa Fluor 647-conjugated secondary antibodies were purchased from Thermo Fisher. HRP-conjugated anti-HA and anti-FLAG primary antibodies were purchased from Roche and Sigma. The ECL detection kit was purchased from Thermo Fisher.

### 2.7 Co-immunoprecipitation (Co-IP) assay

$2 \times 10^6$  293T cells were seeded in 10 cm culture dishes and transfected 12 h later. Forty-eight hours post-transfection, the cells were lysed with RIPA buffer and cleared by centrifugation. The supernatants were collected and incubated with anti-FLAG antibody-conjugated magnetic beads (Sigma) overnight at 4°C. Then, the beads were collected with a magnetic rack, repeatedly washed, and used for the WB assay.

## 2.8 Viral infectivity assay

$5 \times 10^5$  293T cells were seeded in 6-well plates 12 h before transfection. 293T cells were co-transfected with pcDNA3.1-FLAG-GP- $\Delta$ MLD/VSV-G, pNL-Luc- $\Delta$ Env, and MARCH expression vectors. Forty-eight hours post-transfection, virion-containing supernatants were collected to infect the indicator Vero cells. Before infection, supernatants were subjected to ultracentrifugation at  $40000 \times g$  for 1 h, and pellets were used for WB or P24<sup>Gag</sup> ELISA quantity assay. Thirty-six hours post-infection, Vero cells were lysed, and viral infectivity was assessed via luciferase activity assay.

## 2.9 Luciferase activity assay

One day before viral infection,  $1 \times 10^4$  Vero cells were seeded in 96-well plates. Virion-containing supernatants were then added to Vero cells. After 48 h, the cell culture was terminated. Cells were washed with PBS 3 times and lysed with 100  $\mu$ L of RIPA buffer. 100  $\mu$ L of cell lysate was taken, mixed with an equal amount of substrate (Bright-Glo luciferase assay system, Promega) for 10 min at RT, and used for luminescence activity measurement.

## 3 RESULTS

### 3.1 Human MARCH1 and MARCH2 inhibited EBOV GP proteolytic processing

Human MARCH1 and MARCH2 showed antiviral activities (26-28), and human MARCH8 could suppress EBOV GP proteolytic processing (29, 30). Thus, in this study, we aim to test whether mammalian MARCH1 and MARCH2 could block EBOV GP cleavage. Sequence alignment indicated MARCH1 shared a high, whereas MARCH2 was a low homology to MRAH8 (Fig. 1). However, they all shared a similar membrane-associated structure (23). We cloned MARCH1 and MARCH2 from humans, cattle, and mice. We then trace these mammalian MARCH proteins' intracellular distribution. We inserted a green fluorescent protein (GFP) tag in these MARCH proteins' C-terminus. Confocal analysis indicated that these MARCH proteins showed membrane-associated and scattered punctate distribution (Fig. 2A), similar to the intracellular localization of MARCH8 as previously reported (29). Next, we detected the anti-EBOV GP activity of these MARCH proteins. As shown in Fig. 2B, similar to humans MARCH8, MARCH1 and MARCH2 also suppressed GP processing. Similarly, bovine MARCH2 and murine MARCH1 could block GP cleavage (Fig. 2B). Intriguingly, murine MARCH2 nearly lost such inhibition effects. Notably, in the presence of bovine MARCH1, both GP<sub>0</sub> and GP<sub>1</sub> expression was significantly impaired (Fig. 2B), which differed from the other MARCH proteins' antiviral pattern. We then applied the GP- $\Delta$ MLD-mediated pseudovirus infection system to check whether these MARCH proteins could block viral replication (29). Compared to the vector control group, viral infectivity was significantly suppressed in the presence of the MARCH proteins except the murine MARCH2 (Fig. 2C), which matched their blocking effects on GP cleavage. Therefore, these results demonstrated that human/murine MARCH1 and human/bovine MARCH2 blocked EBOV GP proteolytic processing. In addition, human MARCH1 and MARCH2 also inhibited VSV-G pseudotyped virion infectivity (Fig. 2D) and suppressed EBOV GP cleavage in human liver Huh-7 cells (Fig. 2E).

### 3.2 Human MARCH1 and MARCH2 retained EBOV GP in the TGN apparatus.

Generally, mature GP<sub>1,2</sub> is presented on the cell surface, enveloped into virions, and responsible for binding target cells' receptors in EBOV next round of infection. Human MARCH1 and MARCH2 reduced both GP<sub>1</sub> expression and GP<sub>1,2</sub>-mediated viral infectivity. We thus deduced that human MARCH1 and MARCH2 downregulated GP<sub>1</sub> cell surface display. To confirm the hypothesis, the GP- $\Delta$ MLD-GFP was co-transfected with human MARCH1 or MARCH2. GP- $\Delta$ MLD-GFP displayed a plasma membrane (PM) localization, and the human MARCH1 and MARCH2 proteins showed scattered punctate distribution (Fig. 3A). In the presence of human MARCH1 or MARCH2, the GP- $\Delta$ MLD-GFP protein was downregulated from PM and was retained intracellularly (Fig. 3A). This evidence demonstrated MARCH1 and MARCH2 trapped GP- $\Delta$ MLD-GFP at an intracellular compartment, where it was unable to be transported to PM. To further verify this, we introduced the bimolecular fluorescence complementation (BiFC) system to determine where the GP was retained. MARCH proteins were fused with the Venus N-terminus (VN, residues 2-173)

in their C-terminus, while the GP- $\Delta$ MLD was fused with the Venus C-terminus (VC, residues 154-238) in its C-terminus. Simultaneously, we applied the calnexin-mCherry (CNX-mCherry) and TGN46-mCherry (TGN-mCherry) as the ER and TGN localization markers, respectively (29). MARCH1-VN/MARCH2-VN/MARCH8-VN and GP- $\Delta$ MLD-VC were co-transfected with CNX-mCherry or TGN-mCherry to trace their intracellular localization. Individual MARCH1-VN/MARCH2-VN/MARCH8-VN/GP- $\Delta$ MLD-VC was negative for any fluorescent signals (data not shown). In the presence of MARCH1/2/8, EBOV GP- $\Delta$ MLD was trapped intracellularly, consistent with the former results (Fig. 3B). Further detection indicated MARCH1-VN/MARCH2-VN/MARCH8-VN and GP- $\Delta$ MLD-VC pair groups showed minimal overlap with CNX-mCherry but displayed a strong co-localization with TGN-mCherry (Fig. 3B). Therefore, we concluded MARCH1 and MARCH2 retained GP in TGN, as MARCH8 did.

### 3.3 MARCH1 and MARCH2 inhibited furin-mediated cleavage of EBOV GP

MARCH8 suppressed furin-mediated cleavage of EBOV GP (29). Therefore, based on the above results (Fig. 2B), we further verified whether MARCH1 and MARCH2 could block furin-mediated GP cleavage. We first applied the BiFC system to detect MARCH1/MARCH2/MARCH8 and furin intracellular interaction. MARCH1-VN/MARCH2-VN/MARCH8-VN and furin-VC (FR-VC) were co-transfected into 293T cells. Flow cytometry analysis showed MARCH1-VN/MARCH2-VN/MARCH8-VN, and FR-VC had strong intracellular interaction signals (Fig. 4A). Then, MARCH1-VN/MARCH2-VN/MARCH8-VN and FR-VC were co-transfected into HeLa cells. As indicated in Fig. 4B, these MARCH proteins and furin had a clear intracellular co-localization. Next, to confirm their intracellular interactions, the Co-IP assay was performed. The furin expression vector was co-transfected with MARCH1/MARCH2 and EBOV GP- $\Delta$ MLD expression vectors to further verify furin's binding to MARCH proteins and EBOV GP. As shown in Fig. 4C, MARCH1/2, and GP- $\Delta$ MLD could be co-immunoprecipitated by furin, indicating they formed an intracellular complex, similar to the results obtained in MARCH8, as previously identified (29). Relying on their intracellular interactions, we identify whether these MARCH proteins blocked furin-mediated GP cleavage. Generally, mature GP<sub>0</sub> was cleaved into GP<sub>1</sub> (~130 kDa) and GP<sub>2</sub> (~26 kDa) by endogenous furin, whereas in the presence of exogenous furin overexpression, mature GP<sub>0</sub> was cleaved into three parts, i.e., the GP<sub>1</sub>, GP<sub>1</sub><sup>\*</sup> and GP<sub>2</sub> (Fig. 4D, lane 2), as previously demonstrated (29). Full-length GP was co-transfected with furin in the absence or presence of these MARCH proteins. In the presence of MARCH1, MARCH2, or MARCH8, furin-mediated GP cleavage was inhibited because very few GP<sub>1</sub>, GP<sub>1</sub><sup>\*</sup>, and GP<sub>2</sub> were produced (Fig. 4D, lane 3/4/5). Thus, these results demonstrated MARCH1, MARCH2, and MARCH8 could inhibit furin-mediated GP cleavage.

### 3.4 Human MARCH1, MARCH2, and MARCH8 recognized Furin P domain

As the Co-IP assay and flow cytometry analysis indicated (Fig. 4A and C), MARCH1, MARCH2, and MARCH8 interacted with furin. Furin CD and P domains are critically important for substrate cleavage. To identify which domain was necessary for recognition by human MARCH1, MARCH2, and MARCH8, we utilized two previously created furin mutants (29), i.e., the furin CD deletion mutant (FR $\Delta$ CD) and the furin P deletion mutant (FR $\Delta$ P), to perform Co-IP assay with these MARCH proteins. As shown in Fig. 5, MARCH1, MARCH2, and MARCH8 could bind to both full-length furin and the FR $\Delta$ CD but rarely recognize the FR $\Delta$ P, implying these MARCH proteins recognize furin P domain.

## 4 DISCUSSION

MARCH proteins have recently been shown to inhibit viral infections by targeting their envelope glycoproteins. Generally, MARCH proteins exerted their antiviral functions through two different modes, i.e., the pattern of CTD or CTI. Human MARCH8 blocked EBOV GP and SARS-CoV-2 S glycoprotein processing and glycosylation maturation through the CTI antiviral mode (29, 30). Recent work also indicated human MARCH1, MARCH2, and MARCH8 inhibited HIV-1, RABV, and many other viral infections (26-28); mice MARCH1 and MARCH8 suppressed MLV and other viral infection (27). This study further verified human MARCH1 and MARCH2, bovine MARCH2, and murine MARCH1 suppressed EBOV GP proteolytic cleavage via the CTI antiviral mode (Fig. 2B), demonstrating the MARCH protein antiviral potency is

conserved across many mammalian species. The unprocessed mature glycosylation EBOV GP<sub>0</sub> is notably larger than GP<sub>1</sub>, as previously demonstrated (29). However, in the presence of human MARCH1/2, bovine MARCH2, and murine MARCH1, the mature glycosylated EBOV GP<sub>0</sub> did not appear (Fig. 2B), indicating these MARCHs also blocked EBOV GP glycosylation maturation besides inhibiting its cleavage.

Like human MARCH8, human MARCH1 and MARCH2 retained EBOV GP at TGN. They blocked its transportation to PM, thus reducing its cell surface presentation (Fig. 3A). MARCH1 displayed a relatively high sequence homology to MARCH8 but not MARCH2 (Fig. 1). However, they all inhibited EBOV GP cleavage, implying protein conformation was critical to these MARCH proteins' CTI antiviral activities. Interestingly, both EBOV GP<sub>0</sub> and GP<sub>1</sub> were devoid of expression in the presence of bovine MARCH1 (Fig. 2B). It is uncertain which step bovine MARCH1 blocked EBOV GP expression, i.e., at the transcription or expression process, and further work is needed to clarify the accurate mechanism. In contrast to its human and bovine paralogue, murine MARCH2 lost its blocking on EBOV GP cleavage (Fig. 2B), similar to a previous report of MARCH2 inactivation in inducing MLV envelope glycoprotein degradation (27). Given the high sequence homology between human and murine MARCH2, it would be expected to identify which domains are critical for their gain or loss of function in the CTI antiviral mode.

Furin cleaves a group of host intracellular proproteins, which regulate many critical biological processes (38). It also could recognize many viral envelope glycoproteins, including HIV-1 Env, EBOV GP, IAV H5N1 HA, and SARS-CoV-2 S (38, 39). Viral glycoproteins cleavage by furin or other PCs is important for their target cell infection. This study demonstrated that human MARCH1, MARCH2, and MARCH8 specifically interacted with furin, thus blocking EBOV GP cleavage (Fig. 4C and D). Therefore, we deduce that other viral glycoproteins or intracellular proproteins that critically rely on furin cleavage should also be sensitive to human MARCH1, MARCH2, and MARCH8 mediated blocking. MARCH1, MARCH2, and MARCH8 retained EBOV GP in TGN (Fig. 3B) and interacted with furin and EBOV GP (Fig. 4C). These lines of evidence proved that MARCH1, MARCH2, and MARCH8 locked the MARCH1/MARCH2/MARCH8-furin-EBOV GP complex in TGN and thereby prevented their anterograde transport to PM, which clarified a conserved CTI antiviral mode among these human MARCH proteins (the antiviral mode is summarized in Fig. 6). Notably, furin is an autocleavage protein, and mature furin is cleaved by itself at TGN or the cell surface and then secreted outside the cells. Our results showed that intracellular furin expression was enhanced in the presence of human MARCH proteins (Fig. 4D, lane 3/4/5), probably because these human MARCH proteins blocked furin autocleavage activity and retained it at TGN, thus leading to its intracellular accumulation.

Besides MARCH8 (29), many host antiviral proteins also targeted furin to block virus replication (40). In this report, we demonstrated that human MARCH1 and MARCH2, and maybe bovine MARCH2 and murine MARCH1, also inhibited furin-mediated cleavage of EBOV GP. Thus, targeting cellular furin or other PCs to restrict enveloped viruses' infections may be a conserved defense mode employed by host antiviral factors and deserves further exploration.

Generally, in pursuit of survival, viruses evolve some viral proteins to combat host cell antiviral factors. For instance, HIV-1 Vpu and Nef could antagonize cellular BST-2 and SERINC5, respectively (41-43); SARS-CoV-2 ORF7a counteracted SERINC5 antiviral effects (44). Though MARCH proteins were proven to inhibit viral replication potently, less viral antagonizing mechanisms have been discovered.

Only recently, Liu et al. reported that the M2 protein of IAV H1N1 could evade MARCH8 induced degradation through its cytoplasmic tail K78/K79 variation (33). Senecavirus A (SVA) 2AB was discovered to induce MARCH8 autophagic degradation (45). MARCH1, MARCH2, and MARCH8 are highly expressed in monocyte-derived macrophages (MDM) (24, 26), which are critical targets for EBOV infection. Thus, to effectively replicate in MDMs, whether EBOV needs to overcome these human MARCH proteins' restriction deserves to be investigated.

## 5 CONCLUSION

In summary, we revealed a conserved CTI antiviral mode employed by mammalian MARCH1/2 proteins

to inhibit EBOV GP furin-mediated cleavage, which provides new insights for current antiviral studies and may facilitate the development of novel antiviral strategies.

## AUTHOR CONTRIBUTIONS

Changqing Yu, Wenbo Tan, and Yu Bai contributed to the concept and design of this work, acquisition, analysis, interpretation of data, and manuscript preparation; Yulong Zhou, Jingbo Zhai, and Mengzhou Xue contributed to analysis, discussion, or acquisition of data; Qiang Liu and Chunfu Zheng contributed to the concept of this work, acquisition of data, images acquisition, analysis and interpretation of data, and manuscript revision. All authors contributed to this study and approved the submitted version.

## ACKNOWLEDGMENTS

We thank professor Kenzo Tokunaga, professor Shuanghui Yin, and Dr. Nan Wang for the reagents, materials, and technical support and assistance. This work was supported by Natural Science Funding Key Program of Yibin Vocational and Technical College (Grant No. ZR22ZD-01), and the Science and Technology Planning Project of Yibin (Grant No. YBZYSC22BK07) to Changqing Yu; the Nanchong Vocational and Technical College for Basic Scientific Research (Grant No. ZRA1904), and the Science and Technology Planning Project of Nanchong (Grant No. 22XCZX0003) to Qiang Liu.

## CONFLICT OF INTEREST STATEMENT

The authors declare that they have no conflict of interests.

## DATA AVAILABILITY STATEMENTS

The datasets used during the study are included in this article, and materials are available from the corresponding author on request.

## REFERENCES

1. Boso G, Kozak CA. Retroviral Restriction Factors and Their Viral Targets: Restriction Strategies and Evolutionary Adaptations. *Microorganisms*. 2020 Dec 11;8(12).
2. Goto E, Ishido S, Sato Y, Ohgimoto S, Ohgimoto K, Nagano-Fujii M, et al. c-MIR, a human E3 ubiquitin ligase, is a functional homolog of herpesvirus proteins MIR1 and MIR2 and has similar activity. *J Biol Chem*. 2003 Apr 25;278(17):14657-68.
3. Bartee E, Mansouri M, Hovey Nerenberg BT, Gouveia K, Fruh K. Downregulation of major histocompatibility complex class I by human ubiquitin ligases related to viral immune evasion proteins. *J Virol*. 2004 Feb;78(3):1109-20.
4. Ohmura-Hoshino M, Matsuki Y, Aoki M, Goto E, Mito M, Uematsu M, et al. Inhibition of MHC class II expression and immune responses by c-MIR. *J Immunol*. 2006 Jul 1;177(1):341-54.
5. Eyster CA, Cole NB, Petersen S, Viswanathan K, Fruh K, Donaldson JG. MARCH ubiquitin ligases alter the itinerary of clathrin-independent cargo from recycling to degradation. *Mol Biol Cell*. 2011 Sep;22(17):3218-30.
6. Fujita H, Iwabu Y, Tokunaga K, Tanaka Y. Membrane-associated RING-CH (MARCH) 8 mediates the ubiquitination and lysosomal degradation of the transferrin receptor. *J Cell Sci*. 2013 Jul 1;126(Pt 13):2798-809.
7. Chen R, Li M, Zhang Y, Zhou Q, Shu HB. The E3 ubiquitin ligase MARCH8 negatively regulates IL-1beta-induced NF-kappaB activation by targeting the IL1RAP coreceptor for ubiquitination and degradation. *Proc Natl Acad Sci U S A*. 2012 Aug 28;109(35):14128-33.

8. Lin H, Gao D, Hu MM, Zhang M, Wu XX, Feng L, et al. MARCH3 attenuates IL-1beta-triggered inflammation by mediating K48-linked polyubiquitination and degradation of IL-1RI. *Proc Natl Acad Sci U S A*. 2018 Dec 4;115(49):12483-8.
9. Lin H, Feng L, Cui KS, Zeng LW, Gao D, Zhang LX, et al. The membrane-associated E3 ubiquitin ligase MARCH3 downregulates the IL-6 receptor and suppresses colitis-associated carcinogenesis. *Cell Mol Immunol*. 2021 Dec;18(12):2648-59.
10. Zheng C. The emerging roles of the MARCH ligases in antiviral innate immunity. *Int J Biol Macromol*. 2021 Feb 28;171:423-7.
11. Lin H, Li S, Shu HB. The Membrane-Associated MARCH E3 Ligase Family: Emerging Roles in Immune Regulation. *Front Immunol*. 2019;10:1751.
12. Yang X, Shi C, Li H, Shen S, Su C, Yin H. MARCH8 attenuates cGAS-mediated innate immune responses through ubiquitylation. *Sci Signal*. 2022 May 3;15(732):eabk3067.
13. Jin S, Cui J. BST2 inhibits type I IFN (interferon) signaling by accelerating MAVS degradation through CALCOCO2-directed autophagy. *Autophagy*. 2018;14(1):171-2.
14. Kong N, Shan T, Wang H, Jiao Y, Zuo Y, Li L, et al. BST2 suppresses porcine epidemic diarrhea virus replication by targeting and degrading virus nucleocapsid protein with selective autophagy. *Autophagy*. 2020 Oct;16(10):1737-52.
15. Zhai X, Kong N, Zhang Y, Song Y, Qin W, Yang X, et al. N protein of PEDV plays chess game with host proteins by selective autophagy. *Autophagy*. 2023 Mar 2:1-15.
16. Oh J, Wu N, Baravalle G, Cohn B, Ma J, Lo B, et al. MARCH1-mediated MHCII ubiquitination promotes dendritic cell selection of natural regulatory T cells. *J Exp Med*. 2013 Jun 3;210(6):1069-77.
17. Wu J, Xia L, Yao X, Yu X, Tumas KC, Sun W, et al. The E3 ubiquitin ligase MARCH1 regulates antimalaria immunity through interferon signaling and T cell activation. *Proc Natl Acad Sci U S A*. 2020 Jul 14;117(28):16567-78.
18. Nakamura N, Fukuda H, Kato A, Hirose S. MARCH-II is a syntaxin-6-binding protein involved in endosomal trafficking. *Mol Biol Cell*. 2005 Apr;16(4):1696-710.
19. Yoo W, Cho EB, Kim S, Yoon JB. The E3 ubiquitin ligase MARCH2 regulates ERGIC3-dependent trafficking of secretory proteins. *J Biol Chem*. 2019 Jul 12;294(28):10900-12.
20. Xia D, Qu L, Li G, Hongdu B, Xu C, Lin X, et al. MARCH2 regulates autophagy by promoting CFTR ubiquitination and degradation and PIK3CA-AKT-MTOR signaling. *Autophagy*. 2016 Sep;12(9):1614-30.
21. Chathuranga K, Kim TH, Lee H, Park JS, Kim JH, Chathuranga WAG, et al. Negative regulation of NEMO signaling by the ubiquitin E3 ligase MARCH2. *EMBO J*. 2020 Nov 2;39(21):e105139.
22. Zheng C, Tang YD. When MARCH family proteins meet viral infections. *Virol J*. 2021 Mar 2;18(1):49.
23. Tada T, Zhang Y, Fujita H, Tokunaga K. MARCH8: the tie that binds to viruses. *FEBS J*. 2022 Jul;289(13):3642-54.
24. Tada T, Zhang Y, Koyama T, Tobiume M, Tsunetsugu-Yokota Y, Yamaoka S, et al. MARCH8 inhibits HIV-1 infection by reducing virion incorporation of envelope glycoproteins. *Nat Med*. 2015 Dec;21(12):1502-7.
25. Zhang Y, Lu J, Liu X. MARCH2 is upregulated in HIV-1 infection and inhibits HIV-1 production through envelope protein translocation or degradation. *Virology*. 2018 May;518:293-300.
26. Zhang Y, Tada T, Ozono S, Yao W, Tanaka M, Yamaoka S, et al. Membrane-associated RING-CH (MARCH) 1 and 2 are MARCH family members that inhibit HIV-1 infection. *J Biol Chem*. 2019 Mar

8;294(10):3397-405.

27. Umthong S, Lynch B, Timilsina U, Waxman B, Ivey EB, Stavrou S. Elucidating the Antiviral Mechanism of Different MARCH Factors. *mBio*. 2021 Mar 2;12(2).

28. Zhang Y, Ozono S, Tada T, Tobiume M, Kameoka M, Kishigami S, et al. MARCH8 Targets Cytoplasmic Lysine Residues of Various Viral Envelope Glycoproteins. *Microbiol Spectr*. 2022 Feb 23;10(1):e0061821.

29. Yu C, Li S, Zhang X, Khan I, Ahmad I, Zhou Y, et al. MARCH8 Inhibits Ebola Virus Glycoprotein, Human Immunodeficiency Virus Type 1 Envelope Glycoprotein, and Avian Influenza Virus H5N1 Hemagglutinin Maturation. *mBio*. 2020 Sep 15;11(5).

30. Lun CM, Waheed AA, Majadly A, Powell N, Freed EO. Mechanism of Viral Glycoprotein Targeting by Membrane-Associated RING-CH Proteins. *mBio*. 2021 Mar 16;12(2).

31. Villalon-Letelier F, Brooks AG, Londrigan SL, Reading PC. MARCH8 Restricts Influenza A Virus Infectivity but Does Not Downregulate Viral Glycoprotein Expression at the Surface of Infected Cells. *mBio*. 2021 Oct 26;12(5):e0148421.

32. Li C, Shi L, Gao Y, Lu Y, Ye J, Liu X. HSC70 Inhibits Spring Viremia of Carp Virus Replication by Inducing MARCH8-Mediated Lysosomal Degradation of G Protein. *Front Immunol*. 2021;12:724403.

33. Liu X, Xu F, Ren L, Zhao F, Huang Y, Wei L, et al. MARCH8 inhibits influenza A virus infection by targeting viral M2 protein for ubiquitination-dependent degradation in lysosomes. *Nat Commun*. 2021 Jul 20;12(1):4427.

34. Kumar S, Barouch-Bentov R, Xiao F, Schor S, Pu S, Biquand E, et al. MARCH8 Ubiquitinates the Hepatitis C Virus Nonstructural 2 Protein and Mediates Viral Envelopment. *Cell Rep*. 2019 Feb 12;26(7):1800-14 e5.

35. Zhang Y, Tada T, Ozono S, Kishigami S, Fujita H, Tokunaga K. MARCH8 inhibits viral infection by two different mechanisms. *Elife*. 2020 Aug 11;9.

36. Volchkov VE, Feldmann H, Volchkova VA, Klenk HD. Processing of the Ebola virus glycoprotein by the proprotein convertase furin. *Proc Natl Acad Sci U S A*. 1998 May 12;95(10):5762-7.

37. Jeffers SA, Sanders DA, Sanchez A. Covalent modifications of the ebola virus glycoprotein. *Journal of virology*. 2002 Dec;76(24):12463-72.

38. Braun E, Sauter D. Furin-mediated protein processing in infectious diseases and cancer. *Clin Transl Immunology*. 2019;8(8):e1073.

39. Jackson CB, Farzan M, Chen B, Choe H. Mechanisms of SARS-CoV-2 entry into cells. *Nature reviews Molecular cell biology*. 2022 Jan;23(1):3-20.

40. Yu C, Wang G, Liu Q, Zhai J, Xue M, Li Q, et al. Host antiviral factors hijack furin to block SARS-CoV-2, ebola virus, and HIV-1 glycoproteins cleavage. *Emerg Microbes Infect*. 2023 Dec;12(1):2164742.

41. Neil SJ, Zang T, Bieniasz PD. Tetherin inhibits retrovirus release and is antagonized by HIV-1 Vpu. *Nature*. 2008 Jan 24;451(7177):425-30.

42. Rosa A, Chande A, Ziglio S, De Sanctis V, Bertorelli R, Goh SL, et al. HIV-1 Nef promotes infection by excluding SERINC5 from virion incorporation. *Nature*. 2015 Oct 8;526(7572):212-7.

43. Usami Y, Wu Y, Gottlinger HG. SERINC3 and SERINC5 restrict HIV-1 infectivity and are counteracted by Nef. *Nature*. 2015 Oct 8;526(7572):218-23.

44. Timilsina U, Umthong S, Ivey EB, Waxman B, Stavrou S. SARS-CoV-2 ORF7a potently inhibits the antiviral effect of the host factor SERINC5. *Nat Commun*. 2022 May 26;13(1):2935.

45. Sun D, Kong N, Dong S, Chen X, Qin W, Wang H, et al. 2AB protein of Senecavirus A antagonizes selective autophagy and type I interferon production by degrading LC3 and MARCHF8. *Autophagy*. 2022 Aug;18(8):1969-81.

## FIGURE LEGENDS

**Figure 1. Amino acid (aa) sequence alignment of MARCH proteins.** Human MARCH8 aa sequence was aligned with MARCH1 and MARCH2. Dots represent identical aa, while dishes indicate the deletion. M1, human MARCH1; M2, human MARCH2; M8, human MARCH8.

**Figure 2. MARCH proteins blocked EBOV GP cleavage.** A. human/bovine/murine MARCH1/2-GFP and human MARCH8-GFP vectors were transfected into HeLa cells. Nuclei were stained with DAPI, and fluorescent signals were detected by confocal microscopy. B. GP (full-length) was co-expressed with human/bovine/murine MARCH1/2 or human MARCH8 in 293T cells. GP was detected with anti-FLAG, and MARCH proteins were detected with anti-HA. C. GP $\Delta$ MLD, pNL-Luc- $\Delta$ Env, and MARCH expression vectors were co-transfected into 293T cells. Supernatants containing the pseudovirions were collected to infect Vero cells. Infectivity was indicated as luciferase values. D. VSV-G, pNL-Luc- $\Delta$ Env, and human MARCH1/2 expression vectors were co-transfected into 293T cells. Supernatants containing the pseudovirions were collected to infect Vero cells. E. GP (full-length) was co-expressed with human MARCH1/2 in human Huh-7 cells. GP was detected with anti-FLAG, and MARCH proteins were detected with anti-HA. HM, human MARCH; BM, bovine MARCH; MM, murine MARCH; M1, human MARCH1; M2, human MARCH2.

**Figure 3. Intracellular co-localization assay for MARCH proteins and EBOV GP.** A. MARCH1/2 was co-expressed with the GP $\Delta$ MLD-GFP or empty vector in HeLa cells. GP $\Delta$ MLD-GFP was used as a control. MARCH1/2 was detected by anti-HA, and nuclei were stained with DAPI. Fluorescent signals were monitored by confocal microscopy. B. In HeLa cells, the MARCH1/2/8-VN/GP $\Delta$ MLD-VC BiFC pairs were co-expressed with CNX-mCherry or TGN-mCherry, and nuclei were stained with DAPI. Fluorescent signals were collected through confocal microscopy. M1, human MARCH1; M2, human MARCH2; M8, human MARCH8; TGN-MC, TGN-mCherry; CNX-MC, CNX-mCherry.

**Figure 4. MARCH proteins suppressed EBOV GP intracellular cleavage by furin.** A. MARCH1/2/8-VN/furin-VC BiFC pairs were co-transfected into 293T cells. After 36 h, cell samples were collected and pretreated for flow cytometry assay. MARCH8-VN was previously indicated negative for any fluorescent signals (29). B. MARCH1/2/8-VN/furin-VC BiFC pairs were co-transfected into HeLa cells. The MARCH1/2/8-VN proteins were fused with a C-terminal HA tag. Cells were stained with fluorescent anti-HA to detect MARCH proteins and with DAPI to detect nuclei. Fluorescent signals were obtained under confocal microscopy. C. FLAG-tagged furin was co-expressed with HA-tagged MARCH1/2 and HA-tagged GP $\Delta$ MLD proteins in 293T cells. Samples were immunoprecipitated with anti-FLAG and used for WB assay. Furin was detected with anti-FLAG, and MARCH1/2 and GP $\Delta$ MLD were detected by anti-HA. D. GP was co-expressed with furin and MARCH1/2/8. GP and furin were detected by anti-FLAG, and MARCH1/2/8 were detected with anti-HA. FR, furin; M1, human MARCH1; M2, human MARCH2; M8 human MARCH8; SP, signal peptide.

**Figure 5. Critical domain identification of furin interacted with human MARCH1/2/8.** Full-length or Flag-tagged  $\Delta$ CD/ $\Delta$ P furin was co-immunoprecipitated with HA-tagged MARCH1/2/8. Furin was detected with anti-FLAG, and MARCH1/2/8 were detected with anti-HA. M1, human MARCH1; M2, human MARCH2; M8 human MARCH8;  $\Delta$ CD/ $\Delta$ P, furin  $\Delta$ CD/ $\Delta$ P mutant.

**Figure 6. Antiviral model of MARCH molecules in inhibiting EBOV GP maturation.** MARCH proteins were localized in membrane-associated compartments, including ER, TGN, endosomes, and PM. EBOV GP experiences mature glycosylation modification at TGN and is cleaved by Furin into the GP1 and GP2 subunits. The GP1 and GP2 are re-linked and transported from TGN to PM. However, in the presence of MARCH proteins, furin interacted with both MARCHs and EBOV GP and formed the MARCH-furin-EBOV GP complex at TGN. Resultantly, EBOV GP cleavage/glycosylation maturation was blocked and was trapped by MARCH proteins at TGN, which blocked its translocation from TGN to PM. PM, plasma



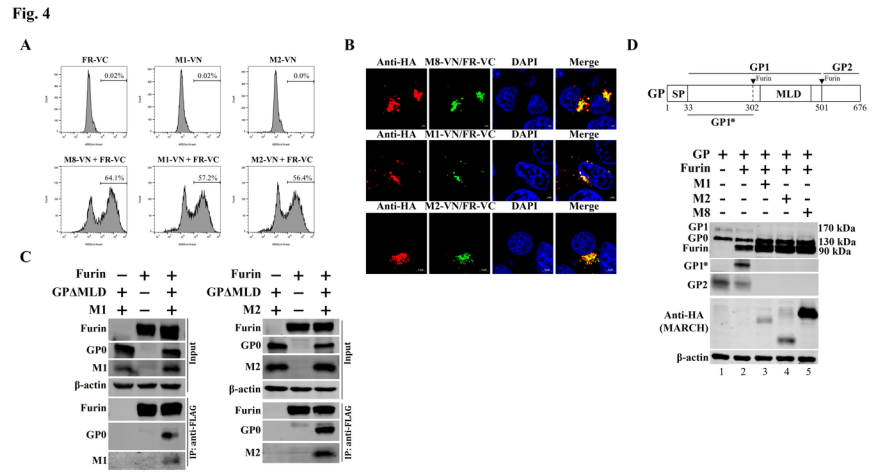
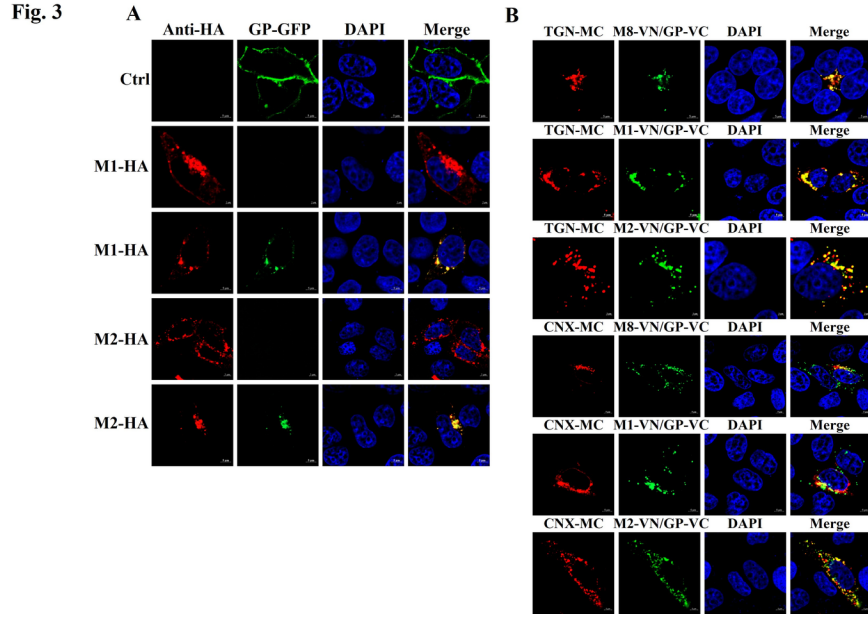


**Fig. 5**

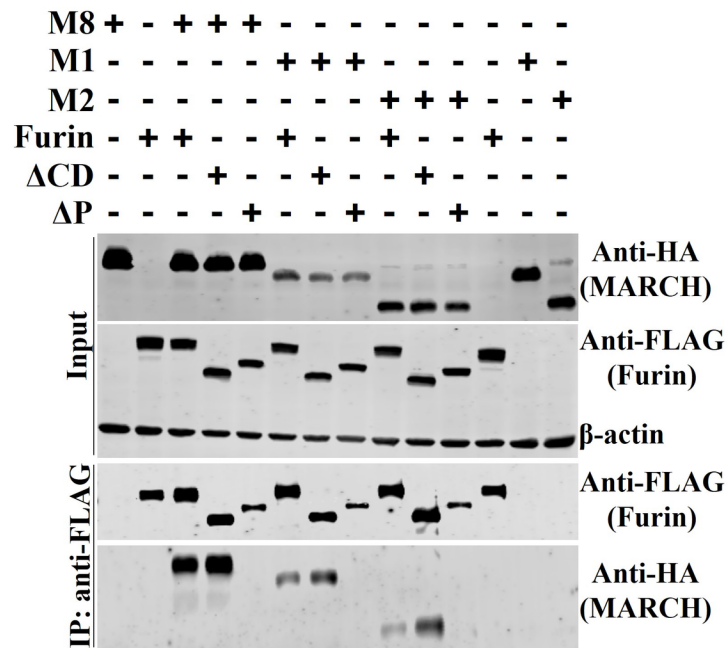


**Fig. 6**

